# Macromolecular Structure and Vibrational Dynamics of Confined Poly(ethylene oxide): from Subnanometer 2-D Intercalation into Graphite Oxide to Surface Adsorption onto Graphene Sheets

| | |
|---|---|
| Journal: | *ACS Macro Letters* |
| Manuscript ID: | Draft |
| Manuscript Type: | Letter |
| Date Submitted by the Author: | n/a |
| Complete List of Authors: | Barroso-Bujans, Fabienne; Centro de Física de Materiales, CSIC-UPV/EHU,<br>Fernandez-Alonso, Felix; Rutherford Appleton Laboratory, ISIS Facility<br>Pomposo, Jose; Materials Physics Centre,<br>Cerveny, Silvina; Consejo Superior de Investigaciones Cientificas, Centro de Fisica de Materiales<br>Alegria, Angel; UNIVERSITY OF THE BASQUE COUNTRY (UPV/EHU), FISICA DE MATERIALES<br>Colmenero, Juan; Universidad del Pais Vasco, Depto. de Fisica de Materiales |
| | |

# Macromolecular Structure and Vibrational Dynamics of Confined Poly(ethylene oxide): from Subnanometer 2D-Intercalation into Graphite Oxide to Surface Adsorption onto Graphene Sheets

Fabienne Barroso-Bujans,*,[1] Felix Fernandez-Alonso,[2,3] José A. Pomposo,[1,4,5] Silvina Cerveny,[1] Angel Alegría,[1,4] and Juan Colmenero[1,4,6]

[1]Centro de Física de Materiales (CSIC, UPV/EHU)-Materials Physics Center, Paseo Manuel de Lardizabal 5, 20018 San Sebastián, Spain

[2]ISIS Facility, Rutherford Appleton Laboratory, Chilton, Didcot, Oxfordshire OX11 0QX, United Kingdom

[3]Department of Physics and Astronomy, University College London, Gower Street, London, WC1E 6BT, United Kingdom

[4]Departamento de Física de Materiales, Universidad del País Vasco (UPV/EHU), Apartado 1072, 20800 San Sebastián, Spain

[5]IKERBASQUE - Basque Foundation for Science, Alameda Urquijo 36, 48011 Bilbao, Spain

[6]Donostia International Physics Center (DIPC), Paseo Manuel de Lardizabal 4, 20018 San Sebastián, Spain

*Supporting Information*

**ABSTRACT:** In this work, high-resolution inelastic neutron scattering (INS) has been used to provide novel insights into the properties of confined poly(ethylene oxide) (PEO) chains. Two limits have been explored in detail, namely, single-layer 2D-polymer intercalation into graphite oxide (GO) and surface polymer adsorption onto thermally reduced and exfoliated graphite oxide, i.e., graphene (G) sheets. Careful control over the degree of GO oxidation and exfoliation reveals three distinct cases of spatial confinement: i) subnanometer 2D-confinement; ii) frustrated absorption and iii) surface immobilization. Case i) results in drastic changes to PEO conformational (800-1000 $cm^{-1}$) and collective (200-600 $cm^{-1}$) vibrational modes as a consequence of a preferentially planar zig-zag (*trans-trans-trans*) chain conformation in the confined polymer phase. These changes give rise to peculiar thermodynamic behavior, whereby confined PEO chains are unable to either crystallize or display a calorimetric glass transition. In case ii), GO is thermally reduced resulting in a disordered *pseudo*-graphitic structure. As a result, we observe minimal PEO absorption owing to a dramatic reduction in the abundance of hydrophilic groups inside the distorted graphitic galleries. In case iii), the INS data unequivocally show that PEO chains adsorb firmly onto the G sheets, with a substantial increase in the population of *gauche* conformers. Well-defined glass and melting transitions associated with the confined polymer phase are recovered in case iii), albeit at sensibly lower temperatures than those of the bulk.

The topological confinement of polymers at the molecular level affects both chain structure and dynamics, and, hence, macroscopic properties. In this context, a sound understanding of the conformational dynamics of single or few-chain polymers in molecular-scale nanodevices is of paramount importance for the development and subsequent deployment of artificial nanomachines mimicking complex biofunctional entities such as enzymes, antibodies, or growth factors. It is well-known that a direct way to confine macromolecules is to place them into a rigid structure with well-defined subnanometer cavities, i.e., under so-called *hard-confinement* conditions. Starting with the works of McKenna and coworkers on the confinement of glass formers within pore glasses,[1, 2] many studies have attempted to provide a physical understanding for the often-observed changes in glass-transition temperature ($T_g$) induced by spatial confinement. Several factors have been invoked as being responsible for differences in structural and dynamical behaviour of confined polymers compared to the bulk. These include geometry (e.g., pore size and shape) as well as specific interfacial interactions (e.g., hydrogen bonding, electrostatic forces, etc.) that can affect in a significant manner both chain conformation and segmental mobility.

In spite of a large body of theoretical and experimental studies on the structure and dynamics of polymers confined into various host materials, it has been difficult to reach a consensus on how purely geometric restrictions and surface interactions influence the micro and mesoscopic properties of the confined phase.[2-5] Typical host materials to effect 2D-confinement include cation-containing layered silicates such as montmorillonite, vermiculite, fluoromica or kaolinite.[6-8] For strongly adsorbing surfaces, indications of a slow-down of the segmental dynamics have been observed, although different trends have also been noted.[5] For weakly adsorbing surfaces, both positive and negative shifts in Tg and relaxation times have also been reported, yet these results still remain quite controversial and largely open to interpretation.[9] As a result, a detailed investigation of the dynamics of polymers confined at subnanometer length scales (<1 nm) in the absence of strong ionic interactions remains largely unexplored, even when theory predicts novel nano-scale effects in transport properties such as *amoeba*-like fluctuations.[10]

Graphite oxide (GO) offers a novel means of studying the structure and dynamics of intercalated molecular and macromo

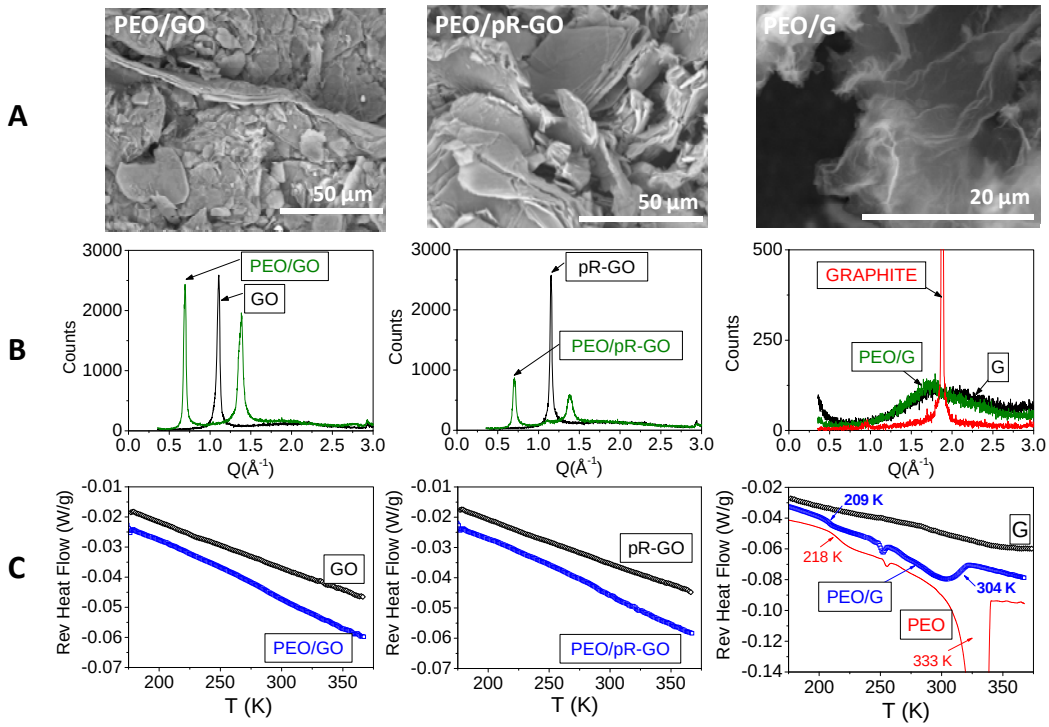


**Figure 1.** A) SEM, B) XRD, and C) TM-DSC measurements of PEO/GO, PEO/pR-GO and PEO/G samples.

lecular species in well-defined *non-ionic* 2D-layers of subnanometer thickness.[11] We have recently studied specific protocols for thermal reduction/exfoliation of pristine GO allowing us to change progressively both the degree of oxidation (DO) and exfoliation (DE) up to highly reduced / exfoliated GO, i.e. graphene (G) sheets.[12] In this work, samples of varying DO and DE were prepared to cover a broad range of GO substrates: from pristine graphite-oxide (GO; high DO/low DE), partially reduced graphite-oxide (pR-GO; medium DO/low DE), reduced graphite-oxide (R-GO; low DO/low DE) to finally neat graphene (G; low DO/high DE). The degree of oxidation in terms of the oxygen to carbon atomic ratio (O/C in at%) in these specimens varied as follows: GO (40) > pR-GO (30) > R-GO (13) ≈ G (13). For more details on the synthesis of GO-based substrates see Supporting Information (SI).

All the above GO-based materials were dispersed in water in the presence of PEO chains (weight average molecular weight, $M_w$ = 94,000 g/mol, polydispersity index, $M_w$ / $M_n$ = 1.08) and stirred at room temperature for 15 days. Excess PEO was subsequently removed by filtration and repeated aqueous washings. The resulting PEO/GO, PEO/pR-GO, PEO/R-GO, and PEO/G materials were dried at 353 K *in vacuo* for 24 h and stored at room temperature under vacuum prior to characterization. Thermogravimetric analysis (TGA) was used to determine the amount of PEO in the samples yielding 27, 21, 2, and 28 wt% for PEO/GO, PEO/pR-GO, PEO/R-GO and PEO/G, respectively (see Table S1).

Scanning electron microscopy (SEM) micrographs illustrate densely packed sheets for PEO/GO, PEO/pR-GO and PEO/R-GO samples, all showing low DE (see Figure 1A, and Figure S3 in SI). Complementary surface-area measurements for GO, pR-GO, and R-GO indicate low BET area values (2 - 7 $m^2/g$), as expected for non-exfoliated materials. Conversely, a fluffy, accordion-like morphology caused by the thermal reduction/exfoliation of GO to yield G sheets was exhibited by the PEO/G sample. G displays a BET surface area as large as 632 $m^2/g$, which is comparable to the values reported in the literature for other graphenes.[13]

X-ray diffraction (XRD) measurements displayed in Figure 1B for PEO/GO and PEO/pR-GO samples show two well-defined (001 and 002) reflections corresponding to an interlayer spacing of 9.1 Å. Hence, PEO chains in these materials are confined to a monolayer of 3.4 – 3.5 Å (i.e. extreme 2D-confinement). This layer thickness is slightly lower than the known interchain distance in bulk PEO (3.9-4.5 Å).[14] In these conditions, the polymer phase exhibits no signs of calorimetric glass or melting transitions in PEO/GO and PEO/pR-GO samples (see Figure 1C), in agreement with previous data for GO with an intermediate degree of oxidation (O/C = 34 at%).[11] Conversely, for the PEO/G sample we observe a relatively broad and weak diffraction feature, corresponding to a characteristic correlation length scale ~3.5 Å, in reasonable agreement with the interlayer distance of pristine graphite (3.4 Å). At first glance, this finding suggests the presence of re-staking phenomena upon reduction of GO. However, BET and SEM measurements indicate that G is a truly exfoliated substrate (in contrast to R-GO). Mechanisms of surface adsorption and immobilization (e.g. based on specific interactions) need to be invoked in order to account for the high PEO uptake by G (28 wt%) when compared to R-GO (2 wt%), the latter displaying *severely frustrated* PEO absorption.

Temperature-modulated differential scanning calorimetry (TM-DSC) measurements (Figure 1C) were consistent with this picture since we found clear signatures of glass (209 K) and melting transitions (304 K) for the PEO/G sample, although these placed at temperatures noticeably lower than those of bulk PEO (218 K and 333 K, respectively). These are key results in order to account for differences between the behavior of a 2D-confined polymer and a polymer adsorbed on a surface. In the first case, all phase transitions associated with the bulk are inhibited because of geometric constraints leading to a lack of cooperativity between vicinal polymer chains. In the second

one, more possibilities exist, including the formation of monolayers, bilayers, bent structures, etc. However, the loss of configurational entropy as well as packing constraints caused by reduction of accessible chain configurations when the macromolecule is in close proximity to an impenetrable wall[15] affects quite noticeably the thermal transitions of the PEO chains, as evidenced by a sensible reduction of both $T_m$ and $T_g$.

To gain further insights into the macromolecular structure of confined PEO, INS measurements on PEO/GO, PEO/pRGO, PEO/G, and their respective substrates were performed on the TOSCA spectrometer at 30 K.[16] One of the primary advantages of INS spectroscopy is that there are no hard selection rules and mode intensities can be directly related to the underlying vibrational density of states (VDOS). Therefore, spectral assignments can be performed on the basis of previous Raman and infrared studies.[17-19] Another advantage of INS spectroscopy to characterize confined hydrogenous materials in GO stems from the strong neutron-proton incoherent cross section which dominates the INS response, with really minimal interference from the GO substrate. This feature has been hardly exploited to date in the study of soft confined matter. Last but not least, INS spectroscopy allows the study of low-energy vibrations below ~200 $cm^{-1}$, difficult to access with infrared and Raman techniques.

A comparison of mass-normalized INS spectra for PEO chains in the bulk, PEO/GO and PEO/G materials is reported in Figure 2. Clearly, the INS spectra of PEO/GO and PEO/G samples are dominated by the response of the polymer phase, thereby greatly simplifying spectral assignment. A detailed assignment of these bands has been reported in Ref. 11. Briefly, the spectral range 800-1000 $cm^{-1}$ is characterized by the presence of $CH_2$ rocking modes (r($CH_2$)), which are particularly sensitive to macromolecular conformation. More specifically, the band at 846 $cm^{-1}$ is a direct fingerprint to *trans-gauche-trans* (tgt) conformations of CCOC, OCCO, and COCC groups in crystalline PEO. These conformations are responsible for the emergence of $7_2$ helical structures in the bulk.[17-19]

In confined PEO (PEO/GO sample), this band moves down to 814 $cm^{-1}$ as a result of the predominance of *trans-trans-trans* (ttt) geometries.[11, 19, 20] Therefore, PEO chains within the GO interlayer display a preferential *ttt* packing in a planar zigzag conformation. This assignment is further corroborated by the red shift and intensity suppression of the spectral feature at 955 $cm^{-1}$, corresponding to *tgt* conformations in the crystal. Lower energy transfers are dominated by collective vibrational modes and also show significant changes in going from the bulk to the confined phase. The bands at 230, 362 and 530 $cm^{-1}$ originate from COC and OCC bending modes coupled to r(CC), r(COC) (230 $cm^{-1}$) and ν(COC) (532 $cm^{-1}$) motions.[17] These features are strongly suppressed in confined PEO. Moreover, the low-energy bands at 115 and 74 $cm^{-1}$ arising from either torsional COC or CO internal rotations are considerably broader in the confined PEO and resemble the vibrational density of states of a disordered amorphous polymer. INS data were found quite insensitive to the degree of oxidation of the underlying GO substrate (see SI). As it is already known that PEO binds to GO via hydrogen bonds, this result is surprising at a first glance, as a higher concentration of oxygen in the substrate should translate into a further reduction in mobility of the confined polymer phase. However, neither the vibrational modes shown in the spectra nor those at higher energy transfers appear to undergo any significant changes. There are two possible explanations for these results: either the differences in the degree of oxidation of these two samples is too small to translate into a significant change in vibrational motions or, alternatively, these vibrational modes are not as sensitive to the presence of hydrogen bonds, but rather to the physical constraints imposed by spatial confinement.

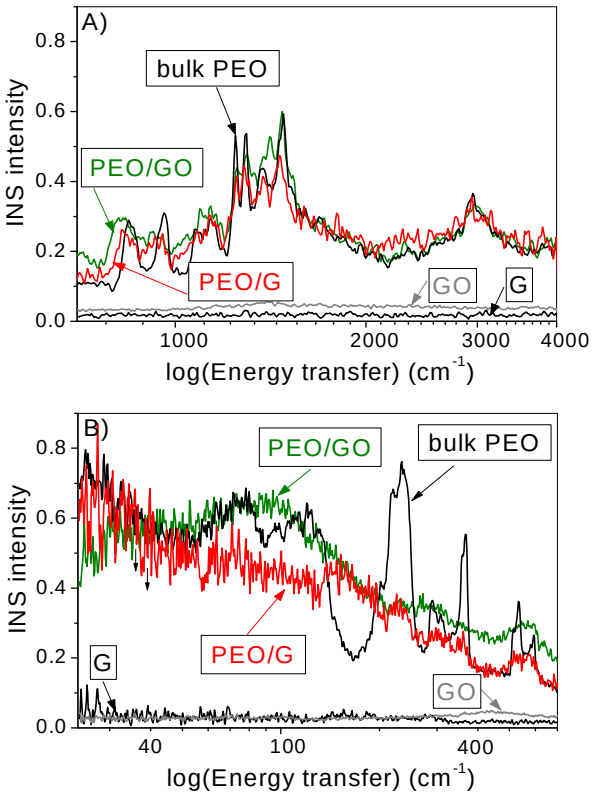


**Figure 2.** A) Mass-normalized INS spectra of PEO in bulk, PEO/GO, and PEO/G. B) Magnification of the low-energy region. INS spectra of both GO and G are also shown for comparison.

In this sense, clear differences are found in the spectrum of PEO/G as compared to that of PEO/GO. In particular, the $CH_2$ rocking band at 814 $cm^{-1}$ in PEO/GO shifts to 835 $cm^{-1}$, an intermediate energy value between that of the confined and the crystalline PEO phase (846 $cm^{-1}$). This spectral shift points to a sensible increase in the population of gauche conformers in PEO/G when compared to PEO/GO.[19] Noticeable differences between both spectra are also found in the region below 400 $cm^{-1}$. This spectral region is dominated by complex collective modes, so-called longitudinal-acoustic modes (LAMs), which are very dependent on the exact sequence of rotameric states.[21] It is noteworthy that the bands at 229, 299, and 360 $cm^{-1}$ also appear in bulk crystalline PEO, but their lower intensity suggests a lower crystallinity degree in PEO/G. These findings are consistent with our TM-DSC experiments (see Figure 1C) showing clear signs of crystal melting in the PEO/G material. Very indicative of the presence of a different polymer phase/layer interacting with the G surface are the appearance of two new bands at 152 and 183 $cm^{-1}$ which were not present in either bulk PEO or in 2D-confined PEO.

To conclude, careful control over the degrees of oxidation and exfoliation of GO substrates and the use of INS spectroscopy in combination with other complementary characterization techniques have enabled for the first time a distinction between three different cases of PEO confinement in GO materials: i)

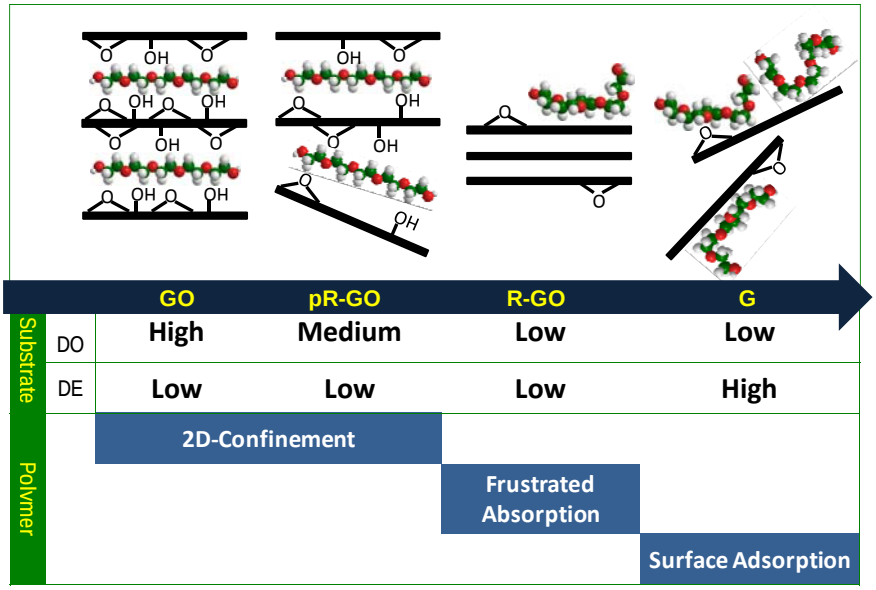


**Figure 3.** Schematic illustration of the conformational state of PEO chains as a function of the degree of oxidation (DO) and exfoliation (DE) of the GO substrate.

extreme 2D-confinement, requiring high DO/low DE or medium DO/low DE; ii) frustrated absorption (low DO/low DE), and iii) surface immobilization (low DO/high DE). Figure 3 summarises these three distinct physical scenarios.

## ASSOCIATED CONTENT

**Supporting Information**. Synthesis and detailed characterization of the materials pertinent to this work, including details on the various experimental techniques. This material is available free of charge via the Internet at http://pubs.acs.org.

## AUTHOR INFORMATION

### Corresponding Author

*E.mail: fbarroso@ehu.es.

### Author Contributions

The manuscript was written through contributions of all authors.

### Notes

The authors declare no competing financial interest.

## ACKNOWLEDGMENT

The support by Spanish Ministry of Education (MAT2007-63681), Basque Government (IT-436-07), Gipuzkoako Foru Aldundia (2011-CIEN-000085-01) and UK Science and Technology Facilities Council is gratefully acknowledged. FBB acknowledges financial support by BERC-MPC. We also thank Dr. A. Larrañaga (SGIker, UPV/EHU) for XRD experiments.

## REFERENCES

(1) Jackson, C. L.; McKenna, G. B. *J. Chem. Phys.* **1990,** 93, 9002-9011.
(2) Alcoutlabi, M.; McKenna, G. B. *J. Phys.: Condens. Matter* **2005,** 17, R461.
(3) Martín, J.; Krutyeva, M.; Monkenbusch, M.; Arbe, A.; Allgaier, J.; Radulescu, A.; Falus, P.; Maiz, J.; Mijangos, C.; Colmenero, J.; Richter, D. *Phys. Rev. Lett.* **2010,** 104, 197801.
(4) Progress in Dynamics in Confinement; Eur. Phys. J. Special Topics. Zorn, R.; van Eijck, L.; Koza, M. M.; Frick, B., Eds.; EDP Sciences, Springer-Verlag, 2010; Vol. 189.
(5) Richert, R. *Annu. Rev. Phys. Chem.* **2011,** 62, 65-84.
(6) Miwa, Y.; Drews, A. R.; Schlick, S. *Macromolecules* **2008,** 41, 4701-4708.
(7) Hackett, E.; Manias, E.; Giannelis, E. P. *Chem. Mater.* **2000,** 12, 2161-2167.
(8) Cerveny, S.; Mattsson, J.; Swenson, J.; Bergman, R. *J. Phys. Chem. B* **2004,** 108, 11596-11603.
(9) Carelli, C.; Young, R. N.; Jones, R. A. L.; Sferrazza, M. *Europhys. Lett.* **2006,** 75, 274-280.
(10) Wittmer, J. P.; Meyer, H.; Johner, A.; Kreer, T.; Baschnagel, J. *Phys. Rev. Lett.* **2010,** 105, 037802.
(11) Barroso-Bujans, F.; Fernandez-Alonso, F.; Cerveny, S.; Parker, S. F.; Alegría, A.; Colmenero, J. *Soft Matter* **2011,** 7, 7173-7176.
(12) Barroso-Bujans, F.; Alegría, A.; Colmenero, J. *J. Phys. Chem. C* **2010,** 114, 21645-21651.
(13) Srinivas, G.; Zhu, Y.; Piner, R.; Skipper, N.; Ellerby, M.; Ruoff, R. *Carbon* **2010,** 48, 630-635.
(14) Johnson, J. A.; Saboungi, M.-L.; Price, D. L.; Ansell, S.; Russell, T. P.; Halley, J. W.; Nielsen, B. *J. Chem. Phys.* **1998,** 109, 7005-7010.
(15) Baschnagel, J.; Binder, K. *Macromolecules* **1995,** 28, 6808-6818.
(16) Colognesi, D.; Celli, M.; Cilloco, F.; Newport, R. J.; Parker, S. F.; Rossi-Albertini, V.; Sacchetti, F.; Tomkinson, J.; Zoppi, M. *Appl. Phys. A: Mater. Sci. Process.* **2002,** 74, s64-s66.
(17) Yoshihara, T.; Tadokoro, H.; Murahashi, S. *J. Chem. Phys.* **1964,** 41, 2902-2911.
(18) Matsuura, H.; Miyazawa, T. *J. Polym. Sci., Part A-2: Polym. Phys* **1969,** 7, 1735-1744.
(19) Maxfield, J.; Shepherd, I. W. *Polymer* **1975,** 16, 505-509.
(20) Papke, B. L.; Ratner, M. A.; Shriver, D. F. *J. Phys. Chem. Solids* **1981,** 42, 493-500.
(21) Yang, X.; Su, Z.; Wu, D.; Hsu, S. L.; Stidham, H. D. *Macromolecules* **1997,** 30, 3796-3802.

Artwork for the Table of Contents